Catal Lett (2009) 128:64–71
DOI 10.1007/s10562-008-9713-0

Composite SBA-15/MFI Type Materials: Preparation, Characterization and Catalytic Performance

Veronika Pashkova · Ewa Włoch · Andrzej Mikołajczyk · Marek Łaniecki · Bogdan Sulikowski · Mirosław Derewiński

Received: 30 July 2008 / Accepted: 26 September 2008 / Published online: 11 November 2008

Abstract SBA-15 type mesoporous molecular sieve was prepared and used as a parent material for synthesis of a SBA-15/zeolite composite. Thus, after addition of an aluminum source into the pristine sample, it was subjected to recrystallization in the water-vapor phase to give the SBA-15/MFI composites. The samples obtained were characterized by XRD, nitrogen sorption, scanning and transmission electron microscopies, ^{27}Al MAS NMR and FT IR. The materials after recrystallization retained their mesoporous character. Characteristics of the material revealed that all the aluminum added was inserted into the final hybrid. As shown by FT IR and NMR, at least some of aluminum was introduced into the nanoparticles of MFI and adopted four-fold coordination, typical for zeolites. Formation of Brønsted acid centres was directly confirmed by IR studies. The catalytic activity was screened in the liquid-phase isomerization of α-pinene. The main products of α-pinene transformations were camphene, limonene and γ-terpinene. The overall selectivity toward camphene + limonene was ca. 90%. Taking into account the low amount of the MFI phase present in a composite sample, calculated initial reaction rate was comparable with other catalytic systems explored in the isomerization of α-pinene.

Keywords SBA-15 · MFI · Composite materials · Porosity · Acidity · Isomerization of α-pinene

1 Introduction

Microporous zeolites (i.e., crystalline aluminosilicates) are a class of materials which focused great attention in the last half century. There are 179 zeolites known, and the list is growing constantly. Their importance stems from the two features: they are characterized by unique architecture of the relatively rigid framework, coupled with the presence of (predominately) Brønsted acid centres. Properly modified zeolites are strong solid acids. However, at variance with other solid-state acids known, for example heteropoly acids [1], the architecture of zeolites gives rise to various pore/cavity systems [2]. These free volumes are occupied by zeolitic water and inorganic and/or organic cations, neutralizing the negative charge of the framework. Upon water removal, the inner space of zeolites becomes available for deposition of species, exerting or modifying catalytic properties. Zeolites are therefore amenable to numerous modifications, focused either on their framework compositions, or species located at the extra framework positions.

Obviously, development of zeolites had a paramount impact on the catalytic processes implemented industrially, starting from cracking, going through transformations of C_8 aromatic hydrocarbons (where shape-selectivity plays a rôle), and ending with numerous applications both in gas and liquid-phases (isomerization, alkylation, etherification, selective oxidation, etc.), to mention a few [3, 4]. Further achievements were made when the more-opened, quasi-zeolitic solids were synthesized, exhibiting regularly arranged array of mesopores. These were MCM type

The work was presented during the conference 'Catalysis for Society', Krakow, May 11–15, 2008.

V. Pashkova · E. Włoch · B. Sulikowski · M. Derewiński (✉)
Institute of Catalysis and Surface Chemistry, Polish Academy of Sciences, Niezapominajek 8, 30-239 Kraków, Poland
e-mail: ncderewi@cyf-kr.edu.pl

A. Mikołajczyk · M. Łaniecki
Department of Chemistry, Adam Mickiewicz University, Grunwaldzka 6, 60-780 Poznań, Poland

materials [5], followed by SBA obtained few years later [6]. Acceleration of fundamental and applied research, not only in catalysis, but in other applications as well, became thus possible. Transport of molecules in such solids was encouraging, and superior to this occurring in standard zeolites.

Recently, successful attempts aimed at coupling the properties of mesoporous materials and zeolites have been undertaken. The route to synthesis of hybrid materials consisting of MCM-41/FAU and MCM-41/MFI were paved by van Bekkum and Urquieta-Gonzáles groups [7–10]. The wormhole-type molecular sieve was also used for preparation of the UL/ZSM-5 composites [11]. Similar strategies were applied later for synthesis of the SBA-15/MFI hybrids [12–14].

Our objective was to prepare and characterize by a number of techniques, the properties of the multimodal porous system, i.e., SBA-15/MFI type materials. SBA-15 was chosen as a mesoporous matrix, due to its enhanced wall thickness and, therefore, better thermal or hydrothermal stability in comparison with MCM-41. The catalytic properties of the composite were screened in the liquid-phase isomerization of α-pinene.

2 Experimental

2.1 Preparation of Composite Materials by Partial Recrystallization of the Amorphous Walls of the Mesoporous Material (SBA-15 type) into the MFI type Microporous Domains

The SBA-15 material is a member of the family of mesoporous solids synthesized in the presence of non-ionic triblock copolymers Pluronic P123 ($EO_{20}PO_{70}EO_{20}$), used as a template. SBA-15 is characterized by the hexagonal pore ordering (hexagonal p6-mm-type structure), pore walls thickness between 3 and 6.4 nm, adjustable pore size and high hydrothermal stability [6, 15]. Synthesis of parent SBA-15 materials was carried out according to the methods described elsewhere [6] in acidic conditions, using Pluronic P123 and tetraethyl orthosilicate (TEOS) as a silica source. In a typical synthesis, 4 g of Pluronic P123 was dissolved in a mixture containing 30 mL of water and 116 mL of 2 M hydrochloric acid solution. Then, 8.5 g of TEOS was added and the solution was stirred at ambient temperature for 20 h. Subsequently, the solution was placed in a stainless steel autoclave and the synthesis was carried out at 105 °C for 24 h. The resultant solid product was washed and dried in air at ambient temperature. Calcination of the as-made SBA-15 material was performed at 500 °C for 6 h in a stream of dry air.

Partial recrystallization of the SBA-15 material was the next step necessary for preparation of a ZSM-5 nano-phase embedded in the mesoporous matrix. Before recrystallization, the calcined sample was impregnated with 1 wt.% water solution of $Al(NO_3)_3 \cdot 9H_2O$, to deliver aluminium source into the mesopores. The amount of the aluminium nitrate was adjusted in such a way as to provide 1 mol% or 2 mol% of Al in relation to Si. After the impregnation, the modified material (SBA-15/xAl, where $x = 1, 2$ denotes 1 or 2 mol% of Al introduced into the solid) was dried at 100 °C and calcined at 200 °C for 18 h. The XRD analysis proved that the impregnation step did not influence the original structure and the porosity of the parent mesoporous solid. Parallel TG experiments gave evidence that major loss of mass (ca. 95%) was observed already upon heating to 200 °C, followed by low mass loss up to 650 °C. The major mass loss was due to desorption of water and decomposition of a nitrate, while the latter one was resulting from dehydroxylation of the sample.

The recrystallization of the pore walls of SBA-15/xAl into the MFI phase was carried out in a vapor phase, according to a procedure adopted from Kang et al. [12]. Thus, the 20 wt.% solution of TPAOH (Aldrich) was diluted further with water and/or ethanol, to yield 10 wt.% solution used for impregnation of the calcined SBA-15/xAl sample. The impregnated samples SBA-15/xAl/TPAOH (Si/TPAOH = 10) were dried at 50 °C for 0.5 h and kept under vacuum overnight to remove water/ethanol from the solid. Subsequently, hydrothermal treatment was carried out. In a standard synthesis, 0.19 g of the dry SBA-15/xAl/TPAOH material was placed in a Teflon holder, necessary to prevent any contact of the solid with liquid water. The holder was placed in a 65 mL volume autoclave containing 0.3 or 0.7 mL of water and the hydrothermal synthesis was carried out at 120 °C for periods varying from 13 to 23 h. The materials obtained were carefully calcined at 500 °C for 8 h in a flow of dry air, applying low heating rate of 1 °C/min to reach the final calcination temperature.

Catalytic tests were carried out in the liquid-phase at 75 °C under atmospheric pressure, using a batch type reactor. Typically, a portion of 100 mg of catalyst was introduced into 2.5 mL of α-pinene (Sigma-Aldrich, 98%), after reaching the reaction temperature. The products were analyzed by a gas chromatograph Hewlett-Packard (5890) equipped with a packed column and a TCD detector.

2.2 Characterization Procedures

Crystallinity and phase purity of the reference and new materials containing the MFI phase was studied using powder XRD (Siemens 5005). The morphology of SBA-15 materials was determined with scanning electron microscopy (SEM) using a Philips XL30 apparatus. The transmission

electron microscopy (TEM) images were recorded using a Philips CM200 instrument. ^{27}Al MAS NMR technique (Bruker 500) was used to study the aluminum environment in the samples. Nitrogen sorption isotherms of the materials obtained were determined at −196 °C using a conventional volumetric technique and a NOVA 2000 sorptiometer (Quantachrome). Prior to analysis, the samples were outgassed under vacuum at 300 °C for 4 h. Acidity of the samples was followed by FT IR spectroscopy, using adsorption of pyridine as a probe molecule. The samples were evacuated at 450 °C for 2 h (10^{-4} Torr) prior measurement.

3 Results and Discussion

3.1 Pure Silica SBA-15

The XRD pattern of the parent, calcined SBA-15 sample is presented in Fig. 1. In the pattern the three well-resolved reflections are seen, which can be indexed as (100), (110) and (200), thus confirming the hexagonally-ordered mesopore system. The SEM analysis reveals that the sample consists of particles of ca. 0.5–1 μm, some of them forming larger, elongated chain-like agglomerates (Fig. 2).

The material gives type IV isotherm of nitrogen according to IUPAC classification, with a typical hysteresis loop. The BET surface area of the sample is 702 m^2/g, with total sorption capacity of $v_{total} = 0.86$ cm^3/g. Analysis of the N_2 sorption isotherm confirms the presence of mesopores. The *t*-plot curve additionally reveals the presence of small amount of micropores, located in the walls of SBA-15. The average pore diameter, calculated form the adsorption branch of isotherm, is equal to 7.6 nm. The wall thickness of the sample, obtained from XRD and sorption data, is ca. 6.0 nm. The well-ordered hexagonal arrangement of mesopores is clearly seen in a TEM micrograph (Fig. 3).

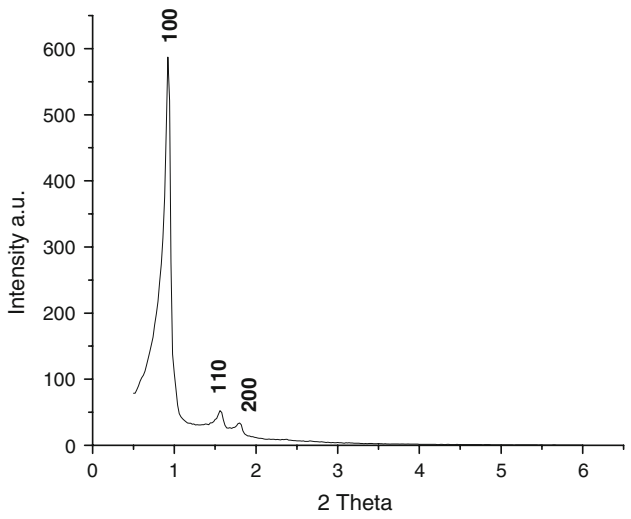

Fig. 1 XRD pattern of the parent, calcined SBA-15 material

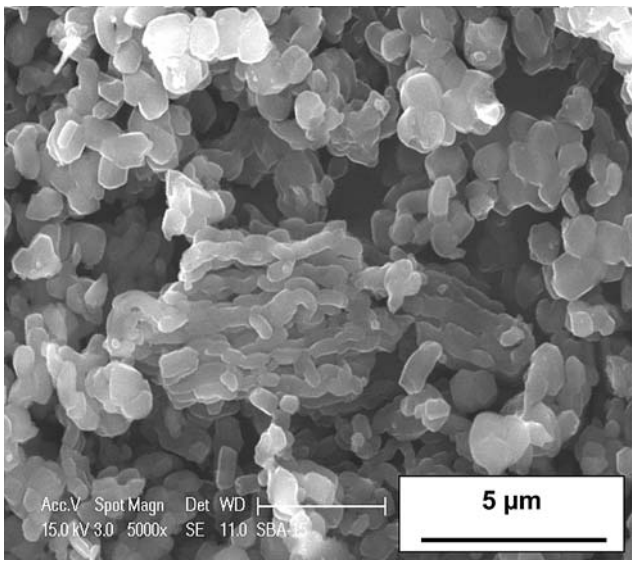

Fig. 2 SEM micrograph of the parent, calcined SBA-15 material

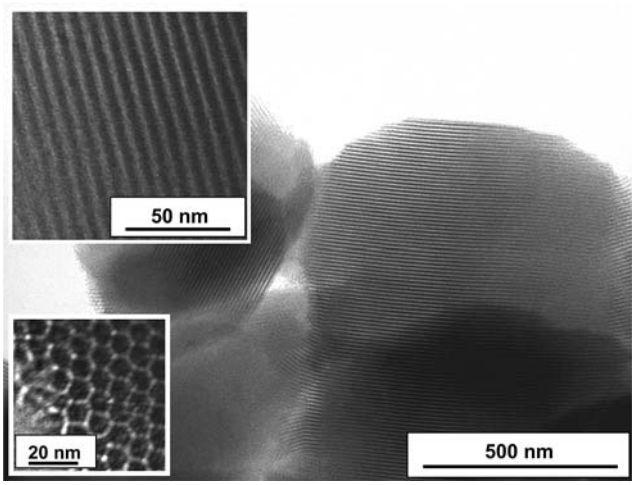

Fig. 3 TEM micrographs of the pure siliceous SBA-15 material

3.2 Modification with Aluminum

Our objective was to generate acid sites in zeolitic material dispersed in the SBA-15 mesoporous matrix. Thus, the first step was to introduce an aluminum source into the purely siliceous SBA-15 sample. In general, there are two possible ways of aluminum insertion. First, Al can be introduced directly during the hydrothermal synthesis of SBA-15. This approach, however, has a disadvantage, because the mesoporous solid containing aluminum inserted during a direct

synthesis, could be significantly disordered. Second, a post-synthesis introduction of aluminum to the already prepared siliceous SBA-15 sample can be accomplished. It was assumed that such a post-synthesis modification with aluminum would enable preparation of a highly-ordered sample.

We note that introduction of 1 or 2 mol% of aluminum affects neither morphology nor size of the Al-impregnated SBA-15 particles. The amount of Al inserted was calculated in such a way as to match the Si/Al ratio required for the synthesis of ZSM-5 (MFI). A detailed TEM analysis confirms no changes in the architecture and the size of mesopores took place upon impregnation with aluminum nitrate. Taking this into account, henceforth we will focus entirely on the sample containing 1 mol% of aluminum (SBA-15/1Al).

The ^{27}Al MAS NMR spectra of SBA-15/1Al give evidence that aluminum is present in extra framework tetra-, penta-, and octahedral coordination, respectively (Fig. 5a). Tetrahedral and octahedral coordination, with essentially the same abundance of the sites, prevails, while a signal corresponding to the pentahedrally-coordinated Al at ca. 35 ppm is in fact weak.

In the next step, the SBA-15/1Al nitrate-free sample was treated with solution of TPAOH at room temperature. A small decrease of the reflection intensities corresponding to the mesoporous phase was found in the XRD spectra of the template-impregnated sample. The minor changes in the mesoporous arrangement were evidenced by close inspection of the TEM micrographs (Fig. 4).

On the other hand, the ^{27}Al MAS NMR revealed a significant change in the state of aluminum. Only tetrahedrally coordinated Al was found in this material, indicating that basic conditions during the template impregnation step

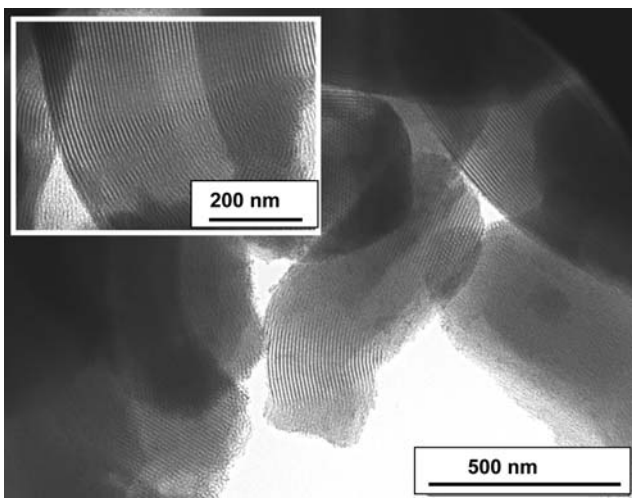

Fig. 4 TEM micrographs of the SBA-15/1Al material impregnated with the structure-directing TPAOH template

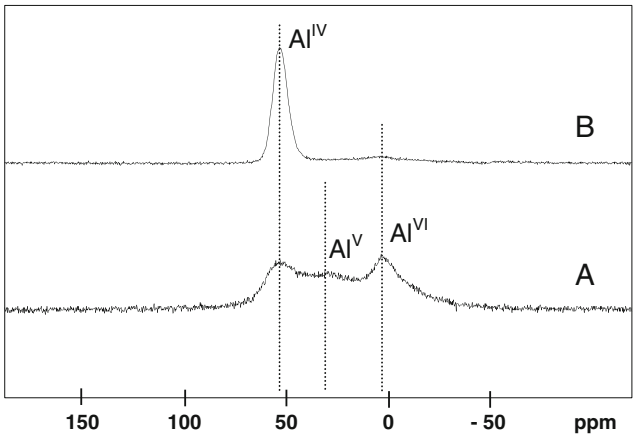

Fig. 5 ^{27}Al MAS NMR spectra of the material before (SBA-15/1Al) (**a**), and after impregnation with the template (SBA-15/1Al/TPAOH) (**b**)

led to almost complete dissolution of aluminum species combined with partial dissolution of the siliceous walls, occurring predominately at the surface. The mutual interaction between the Al and Si species led finally a change of the aluminum environment (i.e., aluminum surrounded predominately by four silicon atoms is experimentally observed (Fig. 5b).

3.3 Composite SBA-15/MFI Material

The template-impregnated SBA-15/1Al sample was dried, evacuated and subjected to the recrystallization, to give a final composite sample (SBA-15/1Al/MFI). During recrystallization partial transformation of the mesoporous material into the microcrystalline phase took place. XRD patterns of the materials obtained after hydrothermal synthesis at 120 °C and sampled at various crystallization times, are shown in Fig. 6. As it is seen, development of the MFI phase occurs already after 13 h of synthesis (Fig. 6a). After this period, the mesoporosity of the parent sample remains almost unchanged. Increasing the synthesis time leads to fast formation of the MFI phase, this is accompanied by gradual disordering of the pristine SBA-15 mesoporous structure (Fig. 6b).

The most interesting composite material is the one containing a well-preserved mesoporous structure coupled with the presence of crystalline, nanosized particles of the ZSM-5 phase. Therefore, we will further discuss data and properties of the materials prepared at crystallization time equal to 16 h.

The HRTEM micrographs of the mesopores system present in the parent SBA-15/1Al and recrystallized SBA-15/1Al/MFI samples are compared in Fig. 7. While a high regularity of the hexagonally-ordered mesopores could be seen in the parent SBA-15/1Al (Fig. 7a), the partial

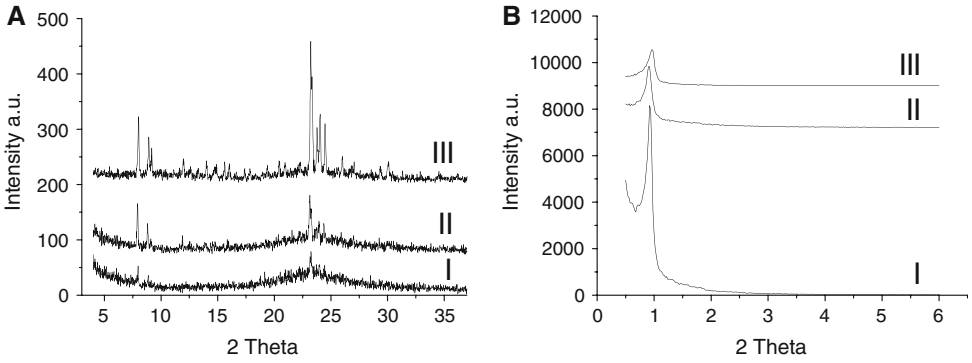

Fig. 6 A comparison of XRD patterns of the SBA-15/1Al/MFI composite materials after 13 h (I), 16 h (II) and 23 h (III) of recrystallization time. The parent SBA-15/1Al sample was impregnated with a water/template-containing solution

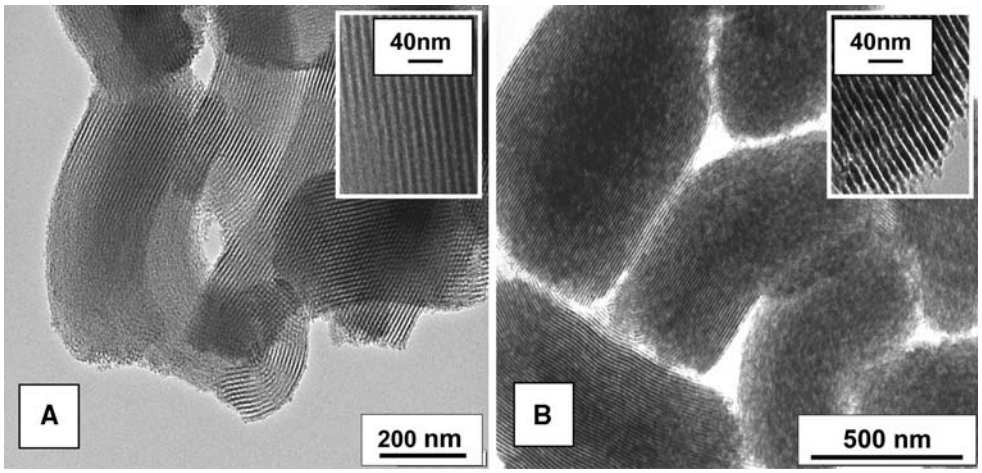

Fig. 7 TEM micrographs of the parent SBA-15/1Al (**a**), and the composite SBA-15/1Al/MFI sample (after 16 h of recrystallization) (**b**)

recrystallization into the MFI nano-domains brought about changes in the walls' thickness (Fig. 7b). However, irrespectively of a small decrease in the pores regularity, the novel material has retained its mesoporous character fully.

The analysis of the SEM micrographs of the SBA-15/1Al/MFI composite revealed that the applied procedure of recrystallization did not affect both the size and morphology of the parent SBA-15 grains. Moreover, close inspection of few tens SEM and TEM micrographs of the composite showed no evidence of the presence of any separated MFI phase. On the other hand, such separated phases were observed if recrystallization was made in the presence of fluoride anions [13] and glycerol–water solution [14]. Changes in the texture of amorphous mesoporous walls after recrystallization, the presence of Al in tetrahedral coordination and generation of acid properties in the composite, all tend to suggest that nano-sized MFI phase was indeed formed. We can therefore conclude that the recrystallization of the walls of the mesopores into the MFI domains was the major process occurring during the hydrothermal treatment.

The nitrogen sorption data of the parent SBA-15 and SBA-15/1Al/MFI composite are shown in Fig. 8. The mesoporous character of pristine SBA-15 is well seen. The isotherm of the material after recrystallization is also of the IVth type, thus indicating no changes in the arrangement of mesopores took place (Fig. 8a). The pore size distribution indicates that mesopores of the parent material shrink slightly upon recrystallization, from 7.6 to 6.5 nm (Fig. 8b). This is probably due to generation of pores irregularity and formation of the bottom-neck type pores, as indicated by analysis of the TEM micrographs (Fig. 9).

Table 1 summarizes N_2 sorption data. First, while the specific surface area decreases by 25%, total pore volume remains almost the same. Simultaneously, a significant increase in the micropore volume is observed (from 0.032 to 0.075 cm^3/g), attributed to the formation of a MFI nanophase with the microporous character.

NMR results indicated formation of 4-coordinated Al in the final composite sample, thus confirmed the presence of Si–O(H)-Al groupings. The presence of Brønsted type acid centres is also directly proved by analyzing the spectra of pyridine adsorbed onto the composite material. After desorption at 150 °C, the strong band of the pyridinium ions at 1,545 cm^{-1}, typical of pyridine bonded to the Brønsted acid centres, is clearly seen (Fig. 10). No acid

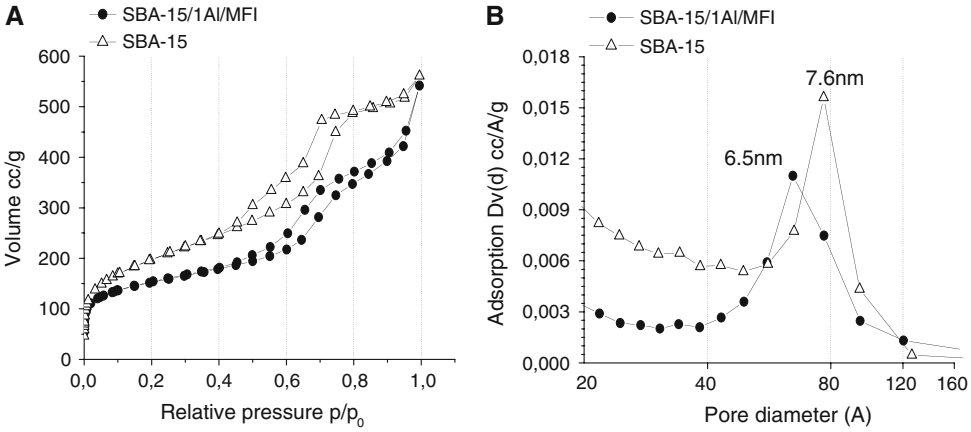

Fig. 8 A comparison of N_2 physisorption isotherms of the parent SBA-15 material and the composite SBA-15/1Al/MFI (after 16 h of the recrystallization) (**a**), and the BJH adsorption pore size distributions of these materials (**b**)

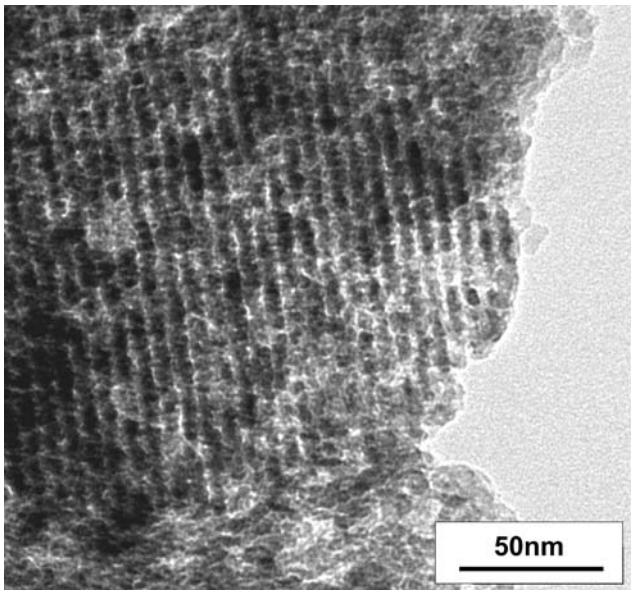

Fig. 9 TEM micrograph of the recrystallized material SBA-15/1Al/MFI

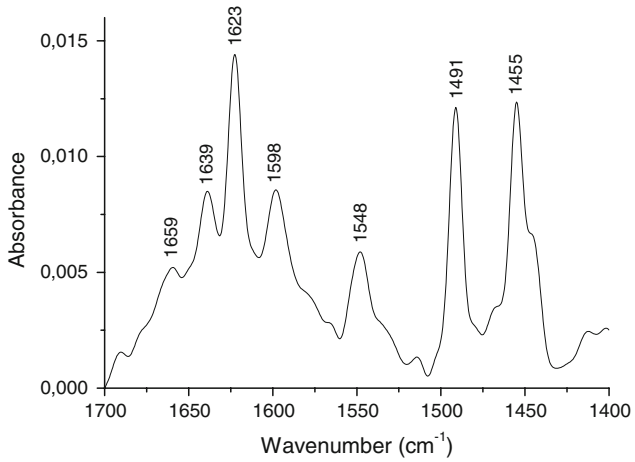

Fig. 10 FT IR difference spectrum of the pyridine adsorbed on the SBA-15/1Al/MFI composite (after 16 h of the recrystallization). Pyridine was desorbed at 150 °C

Table 1 Sorption characteristics for the composite sample SBA-15/1Al/MFI (16 h)

Sample	Specific surface area (m^2/g)	Total pore volume v_{total} (cc/g)	*t*-plot v_{micro} (cc/g)
Parent SBA-15	702	0.86	0.032 (0.057)[a]
Composite SBA-15/1Al/MFI (16 h)	538	0.84	0.075 (0.103)[a]

[a] Calculated by a DFT method

centres were present in the parent sample. The Brønsted acid centres are located in the MFI nanophase, formed in the SBA-15 material upon recrystallization.

To summarize, the new multimodal porous system SBA-15/MFI was obtained, in which an open porosity and easy access to the new active centres present in the nano-domains of the MFI phase are combined together. The partially recrystallized mesoporous molecular sieve could be an interesting candidate for catalytic applications, especially for the transformation of larger molecules than those which can be sorbed by and rearranged over standard zeolites.

α-Pinene is the most abundant member of a large class of terpene hydrocarbons. This compound is an important raw product for flavor & fragrance and pharmaceutical industries [16]. Nowadays, α-pinene is isomerized at the industrial scale towards camphene and limonene, using the acid-impregnated TiO_2 contact [17]. However, due to various limitations of the process carried out using titania, there is still a great interest in developing viable catalysts. Isomerization requires an acidic catalyst, and different contacts were screened for this purpose, including acid-treated oxides, resins, heteropoly acids, clays and zeolites [18].

Table 2 Catalytic data for the isomerization of α-pinene over the SBA-15/1Al/MFI composite, obtained after 16 h of recrystallization. Conditions: temperature 75 °C, $m = 0.1$ g of catalyst, 2.5 mL of the substrate

Reaction time (min)	Conversion of α-pinene (mol%)	Selectivity (%)		
		Camphene	Limonene	γ-Terpinene
5	1.7	37.1	44.3	11.0
15	3.2	38.0	45.2	10.7
30	3.2	38.7	45.7	11.3
60	3.8	39.5	47.6	12.8
90	4.1	45.7	44.0	9.9
120	4.0	45.3	44.2	10.3

The catalytic activity of the parent siliceous SBA-15 material was, as anticipated, negligible (Table 2). Conversion of α-pinene, of the order 0.2–0.3% after 10 and 120 min, was very low, evidently due to the lack of the acid centres in the pristine material, which was used for comparison purpose.

However, when using the SBA-15/1Al/MFI hybrid sample, development of catalytic activity was observed, reaching 3.8% after 60 and 4.0% after 120 min. This is direct evidence that acid centres have been indeed formed in the material, giving rise to catalytic activity, in agreement with IR and NMR studies (cf. *supra*).

Interestingly, the three main products of α-pinene isomerization were: camphene, limonene and γ-terpinene (*p*-cymene and α-terpinene were not formed). The overall selectivity toward camphene and limonene remained essentially constant during reaction times up to 2 h, and was around 90%, i.e., higher than this observed over the ferrierite-type catalysts [18]. As the conversion levels changed from 1.7 to 4.0%, the selectivity to limonene and γ-terpinene remained essentially constant, being equal to ca. 45% and ca. 11%, while the one towards camphene increased slightly (Table 2).

Finally, it is of interest to consider the catalytic data in a more quantitative way. We note that the catalytically active MFI nano-phase, exhibiting the presence of Brønsted acid sites, is only a small fraction of the sample used for the reaction. If we assume that: (i) ca. 5 wt.% of MFI is present in the composite (i.e., a limit of MFI detection by XRD), and (ii) all the aluminum giving rise to Brønsted acidity is located in the MFI nano-phase, then the initial reaction rate could be calculated; the value obtained is 1.95 [mmole α-pinene/($g_{MFI\ phase}$·min)]. This approximate estimation of the initial reaction rates is in a good agreement with the previously calculated data for different classes of catalysts, 0.63–1.42 for HPW-SiO_2, ca. 1.5 for sulphonated ZrO_2, and 2.31–5.01 mmol/g·min for dealuminated ferrierites, respectively [18]. The observed conversion level in the composite is low due to low amount of the MFI phase present in the sample.

4 Conclusions

The composite SBA-15/MFI type materials were obtained by using a dry-gel method. Final recrystallization was performed in the water-vapor phase. The materials obtained retained their mesoporous character, as evidenced by sorption data. Characteristics of the material revealed that essentially all the aluminum added was inserted into the final hybrid (as any separate aluminum phase was not found in the composite). As shown by FT IR and NMR, at least some of aluminum was inserted into the nanoparticles of MFI and adopted four-fold coordination, typical for zeolites. Formation of Brønsted acid centres was directly confirmed by IR studies, and indirectly by studying catalytic properties in the liquid-phase isomerization of α-pinene. We attribute catalytic activity of the composite to the presence of Brønsted acid sites formed in the nanoparticles of the MFI phase. Finally, taking into account the low amount of the MFI phase present in the composite sample, the estimated initial reaction rate was comparable with the other catalysts studied in the title reaction.

Acknowledgment We are grateful to the Ministry of Science and Higher Education, Warsaw, Poland, for support (Grant No. HISZPANIA/139/2006). We also thank Ł. Mokrzycki, MSc, for catalytic tests.

References

1. Okuhara T, Mizuno N, Misono M (1996) Adv Catal 41:113
2. International Zeolite Association web-site: at http://www.iza-online.org
3. Marcilly CR (2000) Top Catal 13:357
4. Clerici MG (2000) Top Catal 13:373
5. Kresge CT, Leonowicz M, Roth WJ, Vartuli JC, Beck JS (1992) Nature 359:710
6. Zhao D, Huo Q, Feng J, Chmelka BF, Stucky GD (1998) J Am Chem Soc 120:6024
7. Kloestra KR, Zandbergen HW, Jansen JC, van Bekkum H (1996) Microporous Mater 6:287
8. Verhoef MJ, Kooyman PJ, van der Waal JC, Rigutto MS, Peters JA, van Bekkum H (2001) Chem Mater 13:683

9. Huang L, Guo W, Deng P, Xue Z, Li O (2000) J Phys Chem B 104:2817
10. Campos AA, Martins L, de Oliveira LL, da Silva CR, Wallau M, Urquieta-Gonzalez EA (2004) Stud Surf Sci Catal 154:541
11. Trong On D, Kaliaguine S (2001) Angew Chem, Int Ed 40:3248
12. Kang K-K, Ahn W-S, Rhee H-K (2004) Stud Surf Sci Catal 154:497
13. Campos AA, Martins L, de Oliveira LL, da Silva CR, Wallau M, Urquieta-González EA (2005) Catal Today 107–108:759
14. Campos AA, Dimitrov L, da Silva CR, Wallau M, Urquieta-González EA (2006) Microporous Mesoporous Mater 95:92
15. Zhao D, Feng J, Huo Q, Melosh N, Fredericson GF, Chmelka BF, Stucky GD (1998) Science 279:548
16. Monteiro JLF, Veloso CO (2004) Top Catal 27:169 2004
17. Gscheidmeier M, Häberlein H, Häberlein HH, Häberlein JT, Häberlein MC (1998) US Patent 5,826,202
18. Rachwalik R, Olejniczak Z, Jiao J, Huang J, Hunger M, Sulikowski B (2007) J Catal 252 161 and references therein